Journal of Power Sources 266 (2014) 347–352

Contents lists available at ScienceDirect

Journal of Power Sources

journal homepage: www.elsevier.com/locate/jpowsour

Short communication

One-step triple-phase interfacial synthesis of polyaniline-coated polypyrrole composite and its application as electrode materials for supercapacitors

Wen Lei [a], Ping He [a,*], Susu Zhang [a], Faqin Dong [a], Yongjun Ma [b]

[a] *State Key Laboratory Cultivation Base for Nonmetal Composites and Functional Materials, School of Materials Science and Engineering, Southwest University of Science and Technology, Mianyang 621010, Sichuan, PR China*
[b] *Analytical and Testing Center, Southwest University of Science and Technology, Mianyang 621010, Sichuan, PR China*

HIGHLIGHTS

- Triple-phase interface synthesis of nanostructured composites was firstly proposed.
- One-step route for the preparation of core–shell PPy/PANI composite was achieved.
- As prepared PPy/PANI composite showed superior capacitance behaviors.

GRAPHICAL ABSTRACT

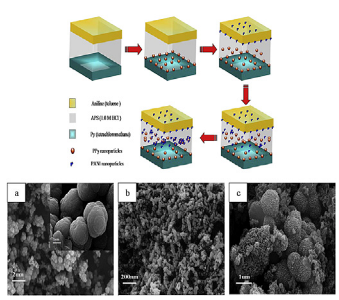

ARTICLE INFO

Article history:
Received 22 February 2014
Received in revised form
11 May 2014
Accepted 12 May 2014
Available online 21 May 2014

Keywords:
Triple-phase interface
Polypyrrole/polyaniline composite
Specific capacitance
Supercapacitors

ABSTRACT

We first present an alternative one-step route for constructing a novel polyaniline (PANI)-coated polypyrrole (PPy) composite in an ingenious triple-phase interface system, where PPy and PANI are prepared in individual non-interference interfaces and, in the middle aqueous phase, smaller PANI particles are uniformly coated on the surface of PPy particles, forming a core–shell structure. The prepared PPy/PANI composite electrode shows a superior capacitance behavior that is more suitable for supercapacitor application.

1. Introduction

Conducting polymers, which mainly include polypyrrole (PPy), polyaniline (PANI), polythiophene and their derivatives, are playing an important role in the construction of high performance supercapacitors due to their high electrical conductivity, environmental stability and consequential redox properties associated with the chain heteroatoms [1]. Normally, the structure of electrode materials is the crucial issue determining the energy storage performance of supercapacitors [2].

Hybrid materials for electrode of supercapacitors have drawn much attention for a long period of time, but the concept of hybrid materials emerged only when research shifted to prepare more sophisticated materials for the purpose of generating desirable properties and functionalities [3].

Electrochemical properties of conducting polymers can be dramatically improved by forming composites between the

* Corresponding author. Tel.: +86 816 6089371.
E-mail addresses: heping@swust.edu.cn, 49416151@qq.com (P. He).

http://dx.doi.org/10.1016/j.jpowsour.2014.05.064
0378-7753/

conducting polymers and with other materials such as carbon materials and metal oxides [4–6]. Once the composition was formed, the integration of composite might combine the merits of each component and yield enhanced properties via synergistic effects [7].

A long standing supercapacitor hypothesis is that more robust nanostructures with abundant hierarchical (meso- and macro-) porosity and large specific surface areas (SSA) will inevitably lead to efficient contact between electrolyte ions and electroactive sites for Faradaic energy storage [8–10]. In addition, electrode materials self-assembled with nano/micro-hierarchical superstructures are one of the best systems in the construction of supercapacitors. The higher level structures assembled from nanometer-sized building blocks offered the advantages of both nanometer-sized building blocks and micro- or submicrometer-sized assemblies. Specifically, the building blocks with high SSA and high surface-to-bulk ratio provide a shorter diffusion path and are the cruxes to benign kinetics and high capacities [11].

Conventional synthesis (electrochemical deposition [12], chemical oxidation [4], etc.) of conducting polymer composites is usually complicated on account of avoiding generating copolymers. Therefore, these methods are always time-consuming and intricate. Electrochemically deposited PANI and PPy show substantial resistivity, probably due to the lack of conducting pathways at the

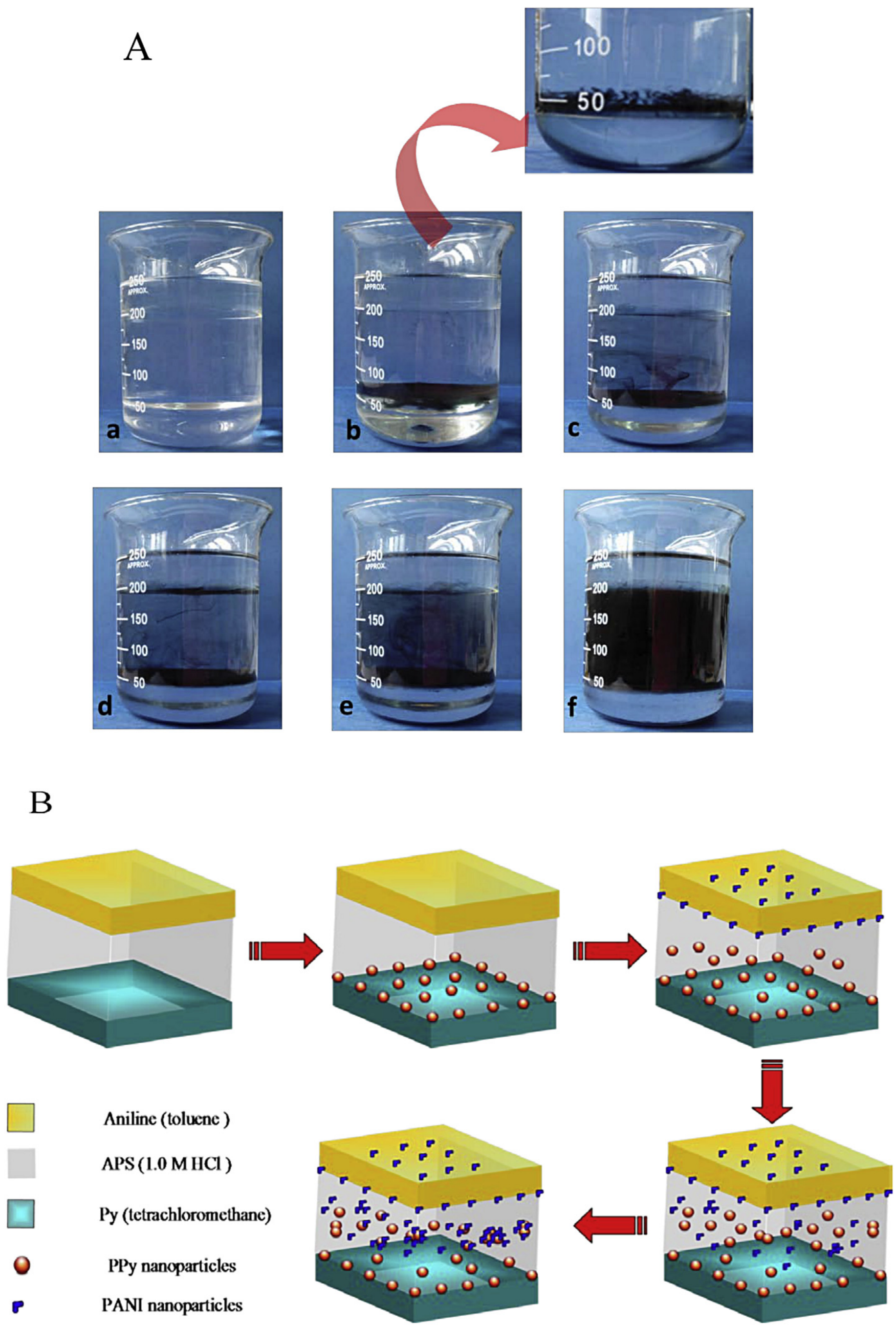

Fig. 1. Photograph illustrations for the synthesis of PPy/PANI composite by a one-step triple-phase interfacial method (A); schematic illustration of interfacial synthesis of PPy/PANI composite (B).

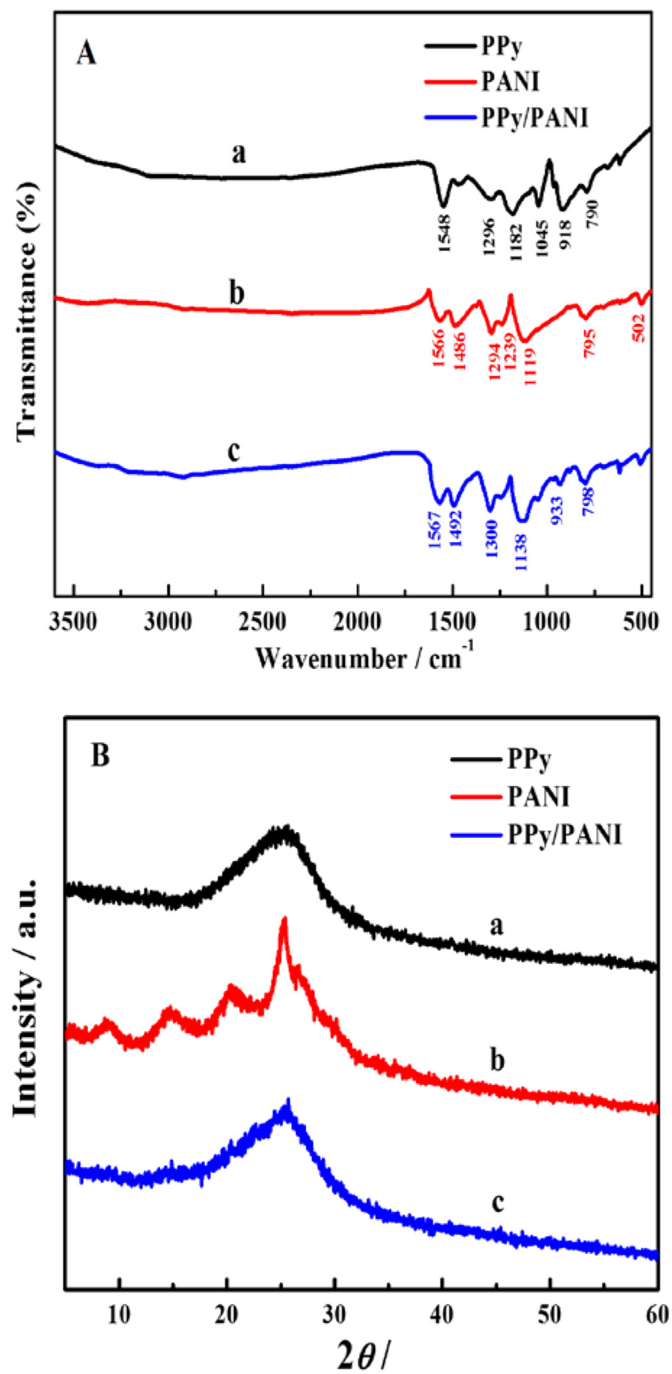

Fig. 2. A: FTIR spectra of PPy (a), PANI (b) and PPy/PANI composite (c); B: XRD patterns of PPy (a), PANI (b) and PPy/PANI composite (c).

nano size level associated with the random deposition morphology. Meanwhile, electrochemical deposition yields thicker deposits of conducting polymer that lead to broader peak in the cyclic voltammogram and thereby present slower kinetics [13]. It is worth mentioning that pyrrole and aniline monomer in the same homogeneous solution always generate copolymers. However, the properties and morphologies of copolymers can not be well controlled, and one major drawback that limits the availability of conductive polymers is the rareness of conjugated π-bond [14]. Mi et al. [4] reported the preparation of core–shell PPy/PANI composite by an in situ chemical oxidation polymerization of aniline on the surface of PPy nanotubes. PPy nanotubes were synthesized by using the complex of methyl orange/$FeCl_3$ as a template as reported [15]. Recently, Liang et al. [16] prepared core–shell PPy/PANI composite by in situ chemical polymerization of pyrrole monomer in the presence of PANI nanofibril seeds for integrating the excellent properties of PPy and PANI. By far, no research reported the preparation of core–shell structured conducting polymer composite by one-step triple-phase interfacial synthesis.

In this paper, we reported a novel one-step route to synthesize PPy/PANI composite by chemical oxidation polymerization in a triple-phase interface system. By dividing the reaction system into three phases, PPy and PANI can be prepared in individual non-interference interfaces in the presence of oxidation in the middle aqueous phase. Original morphologies of both PPy and PANI were well preserved and, under the impetus of thermal energy, smaller interconnected PANI nanoparticles were uniformly wrapped on the surface of PPy microsphere particles, forming a nano/micro-hierarchical superstructure.

2. Experimental

2.1. Synthesis of PPy/PANI composite

PPy/PANI composite was prepared by a one-step triple-phase interfacial reaction at temperature of 0–5 °C. A static organic/aqueous/organic triple-phase interface system was formed as follows. At the bottom of beaker, organic phase was obtained by dissolving 5.0 mmol pyrrole into 50 mL cooled tetrachloromethane (CCl_4). Then, 150 mL cooled HCl aqueous solution (1.0 mol L^{-1}) containing 10 mmol ammonium persulfate was used as the middle aqueous phase. Finally, another organic phase on the upper of beaker was prepared by dissolving 5.0 mmol aniline into 50 mL cooled toluene. Subsequently, the reaction system was placed in an ice-bath to control the temperature below 5 °C for 24 h. Resulting black precipitate was obtained and suction-filtered in air and washed with copious amounts of distilled water and dried in 60 °C overnight.

For comparison, PPy and PANI were synthesized according to the similar procedure above by traditional organic/aqueous interface reaction. The simple PPy/PANI composite (S-PPy/PANI) was prepared by mixing obtained PPy and PANI with ethanol under ultrasonic treatment for 10 min, followed by drying in air for 12 h at 60 °C before further treatment.

2.2. Electrochemical tests

Electrodes for supercapacitors were prepared by mixing electroactive materials with 10 wt.% acetylene black and 5 wt.% polytetrafluoroethylene (PTFE) emulsion to make homogeneous slurry in the presence of absolute ethyl alcohol. The slurry was pressed onto a stainless steel fiber felt with an apparent area of 1 cm^2 under the pressure of 5.0 MPa. The mass load of every electrode is approximately 3 mg. Subsequently, the as prepared electrodes were dried at 80 °C for 24 h before use.

1.0 M H_2SO_4 solution was used as electrolyte in all experiments at room temperature. All electrochemical measurements were carried out by introducing a three-electrode test system using platinum sheet as counter electrode, as prepared electrode as working electrode referred to saturated calomel electrode (SCE) immersed in 1.0 M H_2SO_4. Cyclic voltammetry (CV) and electrochemical impedance spectroscopy (EIS) were performed with PARSTAT 2273 electrochemical workstation (Princeton Applied Research, USA). CV tests were preformed between −0.2 and 0.8 V. Impedance measurements were performed in the frequency range from 100 kHz to 0.01 Hz at open circuit potential with an ac

perturbation of 5 mV. Galvanostatic charge/discharge tests were performed between −0.2 and 0.8 V using CHI 760C electrochemical workstation (CH Instruments, China).

3. Results and discussion

Photograph illustrations and schematic illustration for the synthesis of PPy/PANI composite with nano/micro-hierarchical superstructures by a one-step triple-phase interfacial method were shown in Fig. 1. It was found that, when the triple-phase reaction system was established, some black flocculent products appeared continuously at the organic (CCl_4)/aqueous interface, and the black flocculent products diffused slowly to the upper aqueous phase. Soon afterward, some mazarine products appeared at the organic (toluene)/aqueous interface. As both black and mazarine products were produced continuously in individual non-interference interfaces, they mixed together evenly in the aqueous phase, which then turned into black homogenous solution. During the formation process of nanoparticles at the interface, thermal energy causes spatial fluctuations of the particles, and this energy balance results in a weak interfacial aggregation of nanoparticles [17].

Shown in Fig. 2 were FTIR spectra (Fig. 2A) and XRD patterns (Fig. 2B) of as prepared PPy, PANI and PPy/PANI composite. As for the FTIR spectra, in case of PPy (curve a), the fundamental vibrations of pyrrole ring centered at 1546 and 1473 cm^{-1} were ascribed to antisymmetric and symmetric ring-stretching modes, respectively. In-plane deformation of =–C–H at 1296 and 1182 cm^{-1} and out-of-plane vibration of =–C–H at 918 and 790 cm^{-1} were also observed in these spectra [18]. In case of PANI (curve b), the fundamental vibrations centered at 1566 and 1486 cm^{-1} were ascribed to quinonoid ring stretching and benzenoid ring stretching, and peaks at 502, 795, 1294 cm^{-1} were observed for PANI corresponding to deformation of benzenoid rings, C–C stretching of quinonoids and C–N stretching of secondary aromatic amines, respectively [19,20]. FTIR spectrum of PPy/PANI composite (curve c) reflected the mutual influence of PPy and PANI. Compared with curves a and b, the spectroscopic differences in peak intensity and position revealed that there was an interaction between PPy and PANI instead of a simple blend of these two components.

The XRD pattern of PPy (Fig. 2B(a)) showed a broad asymmetric scattering peak located at 2θ angle around 25°, which was typical of amorphous doped PPy [21,22]. Shown in Fig. 2B(b) was XRD pattern of PANI with characteristic peaks around 2θ values of 15, 20 and 25, corresponding to the reflections of emeraldine salt form [23]. These peaks may be assigned to the scattering from PANI chains at interplanar spacing [24]. Shown in Fig. 2B(c) was XRD pattern of PPy/PANI composite with a broad asymmetric scattering peak at 2θ angle around 25°, which was similar to the XRD pattern of PPy. Smaller interconnected PANI nanoparticles were wrapped on the surface of PPy microsphere particles, forming a nano/micro-hierarchical superstructure. The broad diffraction peaks of PANI disappeared, which was possibly because the hierarchical superstructure had acted as "impurities" to hamper the growth of PANI "crystallites" [25]. Generally speaking, amorphous phase of nano/micro-materials is feasible for the supercapacitor application due to easy penetration of ions through the bulk of active materials [26].

Shown in Fig. 3 were SEM images and TEM images of as prepared PPy, PANI and PPy/PANI composite. It was revealed that PPy presented aggregated spherical particles and the size was within the scope of hundreds nanometer scale to micrometer scale (Fig. 3a). In case of PANI, intertwined tubular like nanoparticles were observed in Fig. 3b. By contrast, observed in Fig. 3c was PPy/PANI composite with typical core–shell structure, where PPy microsphere particles acted as the core, and the interconnected PANI nanoparticles were uniformly coated on the surface of PPy and formed a shell of the composite. Different sizes of PPy and PANI particles formed a nano/micro-hierarchical superstructure.

TEM image of prepared PPy was shown in Fig. 3d, it was found that PPy particles presented spherical shape with fairly smooth surface. The typical TEM image of the prepared PANI nanoparticles was shown in Fig. 3e. It was observed that PANI particles were within nanometric scale and well separated over large area coverage.

Observed in Fig. 3f was the prepared composite with typical core–shell structure, and PPy acted as the "core" via the hard template. The smaller interconnected PANI nanoparticles were coated on the surface of PPy and formed as a shell of the composite.

Shown in Fig. 4a were the CV curves of PPy, PANI, PPy/PANI and S-PPy/PANI electrodes measured in 1.0 M H_2SO_4 electrolyte at scan rate of 5 mV s^{-1}. The CV curve of PPy was a little deviation from a rectangular form, and a pair of redox peaks of PANI near 0.6 V and

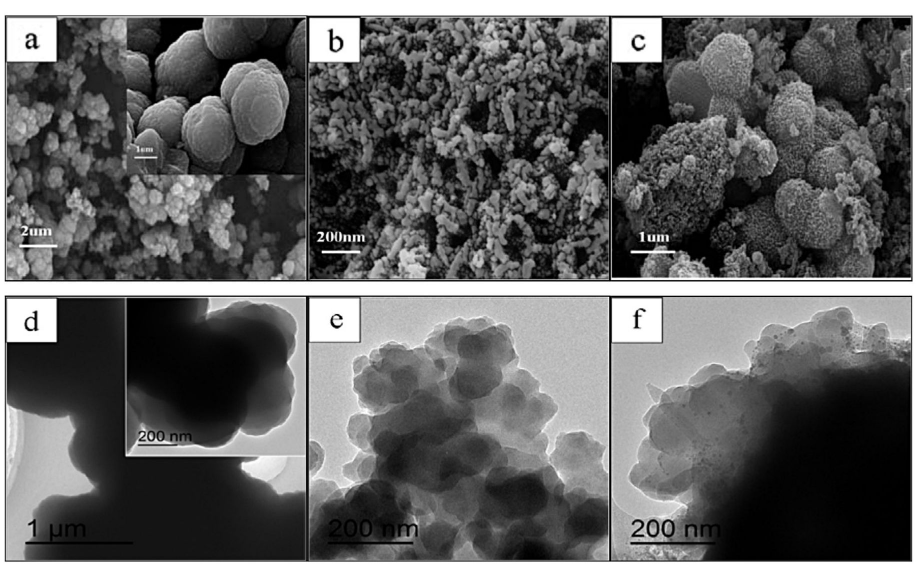

Fig. 3. SEM images of PPy (a), PANI (b) and PPy/PANI composite (c); TEM images of PPy (d), PANI (e) and PPy/PANI composite (f).

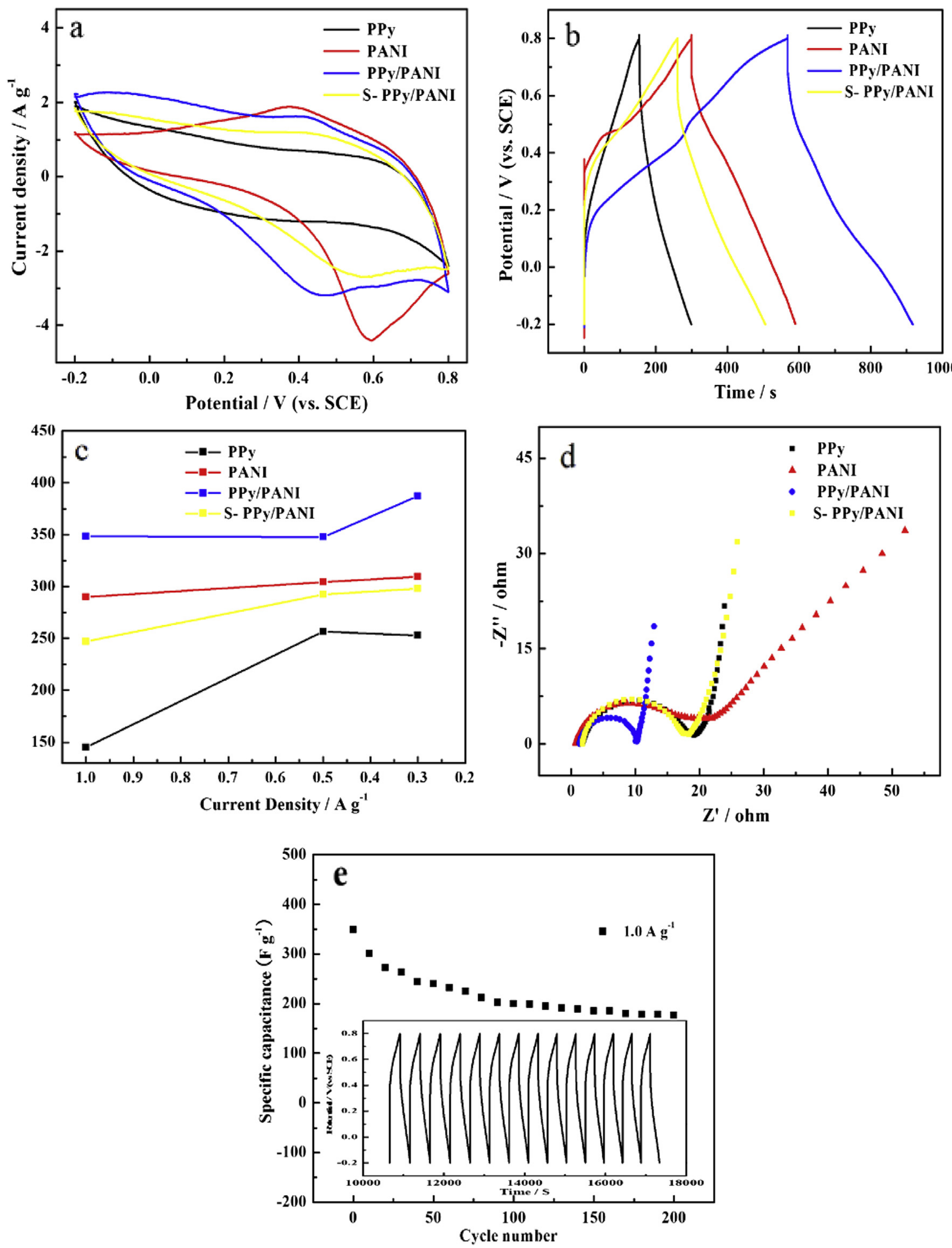

Fig. 4. Cyclic voltammograms of PPy, PANI, PPy/PANI and S-PPy/PANI at scan rate of 5 mV s^{-1} (a); chronopotentiograms of PPy, PANI, PPy/PANI and S-PPy/PANI at current density of 1.0 A g^{-1} (b); specific capacitances of PPy, PANI, PPy/PANI and S-PPy/PANI at different current densities (c); Nyquist plots of PPy, PANI, PPy/PANI and S-PPy/PANI (d); cycle-life of PPy/PANI composite electrode (e).

0.4 V were observed due to the formation of p-benzoquinone/hydroquinone couple [27]. Additionally, the current density and the enclosed area of CV curve of PPy/PANI composite electrode were larger than that of PPy, PANI and S-PPy/PANI, demonstrating a much higher specific capacitance. The enhanced capacitance performances of PPy/PANI composite electrode might be attributed to the positive synergistic effect between PPy and PANI. In this respect, intertwined tubular like PANI nanoparticles are proposed to serve as a protecting layer to maintain the structural integrity of PPy during the bulk redox reaction, which would otherwise weaken the spherical particles due to the harsh and frequent phase variation [3].

Based on Fig. 4b, the calculated specific capacitance of PPy, PANI, PPy/PANI and S-PPy/PANI were 145.0, 290.3, 348.5 and 247.0 F g^{-1}, respectively, at a current density of 1.0 A g^{-1}. It was found that the specific capacitance of S-PPy/PANI was only 71% of that of as prepared PPy/PANI composite. The specific capacitances of as prepared PPy, PANI, PPy/PANI and S-PPy/PANI at current densities of 0.3 and 0.5 A g^{-1} were also calculated (Fig. 4c). PANI exhibited the highest rate-capability, which could be ascribed to its nanoscaled structure. It was well known that controlling the shape and size of nanoparticles can offer some advantages. Such intertwined tubular nanoscaled particles in this work present a large surface area to the electrolyte and can support high rates, although cyclability can be a problem because of structural changes or very reactive surface groups [28]. PPy microsphere particles coated with tubular like PANI nanoparticles effectively formed core–shell structure composite, providing a higher electrochemical active surface area for exploiting the full advantages of PPy and PANI.

The strong interactions in such nano/micro-hierarchical superstructure greatly improved the charge-transfer kinetics process of PPy/PANI composite. Such complex charge transfer reduced the ion intercalation distances to a matter of nanometers and facilitated better charge transfers and lower resistances, which further proved that PPy/PANI composite was more suitable as electrode materials for supercapacitors (Fig. 4d).

Shown in Fig. 4e was the cycle-life of PPy/PANI composite electrode at a current density of 1.0 A g^{-1} in 1.0 M H_2SO_4 solution within the potential range from 0.8 to −0.2 V, and the inset was charge/discharge curves of PPy/PAN composite electrode. The specific capacitance of PPy/PANI composite electrode decreased with cycle number and it remained nearly stable after 100 cycles with the specific capacitance of 180 F g^{-1}, and 51.6% of initial capacitance was retained. The reasons for the non-ideal capacitance behavior can be interpreted as follows. The intrinsic poor cycle stability of conducting polymers was an inevitable factor that should be taken into account [13]. On the other hand, the three-dimensional intercalation and redox reactions occurred in the solid activated materials of electrodes during the charge/discharge process, which might result in the alteration of crystal microstructure or crystalline of electrode materials. The collapse of crystal structures or microspheres of electrode materials during the earlier stage of charge/discharge process might result in the relative instability of specific capacitance [29].

4. Conclusions

In summary, we first proposed an alternative one-step route by constructing a novel hybrid conducting polymers core–shell nanoparticles in a triple-phase interface system. By dividing the reaction system into three phases, PPy and PANI were prepared in individual non-interference interfaces in the presence of oxidation agent in the middle aqueous phase. Original morphologies of both PPy and PANI were well preserved and, under the impetus of thermal energy which caused spatial fluctuations of particles, smaller PANI particles were uniformly coated on the surface of PPy particles, forming nano/micro-hierarchical superstructure. The fabricated PPy/PANI composite electrode showed a superior capacitance behavior that was more suitable for supercapacitor application. This novel triple-phase interface method presented in this work provides a new strategy for the synthesis of nano-structured composite in a convenient way.

Acknowledgments

This work was supported by the Open Project of State Key Laboratory Cultivation Base for Nonmetal Composites and Functional Materials (11zxfk26) and the Postgraduate Innovation Fund Project by Southwest University of Science and Technology (14ycxjj0002). Also we are grateful for the help of Analytical and Testing Center of Southwest University of Science and Technology.

References

[1] P. Simon, Y. Gogotsi, Nat. Mater. 7 (2008) 845–854.
[2] D.W. Wang, F. Li, H.M. Cheng, J. Power Sources 185 (2008) 1563–1568.
[3] J.P. Liu, J. Jiang, C.W. Cheng, H.X. Li, J.X. Zhang, H. Gong, H.J. Fan, Adv. Mater. 23 (2011) 2076–2081.
[4] H.Y. Mi, X.G. Zhang, X.G. Ye, S.D. Yang, J. Power Sources 176 (2008) 403–409.
[5] S. Biswas, L.T. Drzal, Chem. Mater. 22 (2010) 5667–5671.
[6] J. Han, L.Y. Li, P. Fang, R. Guo, J. Phys. Chem. C 116 (2012) 15900–15907.
[7] C.Z. Zhu, J.F. Zhai, D. Wen, S.J. Dong, J. Mater. Chem. 22 (2012) 6300–6306.
[8] Z.H. Wen, J.H. Li, J. Mater. Chem. 19 (2009) 8707–8713.
[9] D. Chen, L.H. Tang, J.H. Li, Chem. Soc. Rev. 39 (2010) 3157–3180.
[10] D.W. Wang, F. Li, M. Liu, G.Q. Lu, H.M. Cheng, Angew. Chem. Int. Ed. 47 (2008) 373–376.
[11] B.R. Duan, Q. Cao, Electrochim. Acta 64 (2012) 154–161.
[12] V. Branzoi, F. Branzoi, L. Pilan, Mater. Chem. Phys. 118 (2009) 197–203.
[13] G.A. Snook, P. Kao, A.S. Best, J. Power Sources 196 (2011) 1–12.
[14] F. Fusalba, D. Belanger, J. Phys. Chem. B 103 (1999) 9044–9054.
[15] X.M. Yang, Z.X. Zhu, T.Y. Dai, Y. Lu, Macromol. Rapid Commun. 26 (2005) 1736–1740.
[16] B.L. Liang, Z.Y. Qin, J.Y. Zhao, Y. Zhang, Z. Zhou, Y.Q. Lu, J. Mater. Chem. A 2 (2014) 2129–2135.
[17] Y. Lin, H. Skaff, T. Emrick, A.D. Dinsmore, T.P. Russell, Science 299 (2003) 226–229.
[18] H.T. Ham, Y.S. Choi, N. Jeong, I.J. Chung, Polymer 46 (2004) 6308–6315.
[19] J.D. Sudha, A. Pich, V.L. Reena, S. Sivakala, H.J.P. Adler, J. Mater. Chem. 21 (2011) 16642–16650.
[20] U. Rana, S. Malik, Chem. Commun. 48 (2012) 10862–10864.
[21] S.P. Palaniappan, P. Manisankar, Mater. Chem. Phys. 122 (2010) 15–17.
[22] X.M. Yang, Y. Lu, Mater. Lett. 59 (2005) 2484–2487.
[23] P. Saini, V. Choudhary, B.P. Singh, R.B. Mathur, S.K. Dhawan, Mater. Chem. Phys. 113 (2009) 919–926.
[24] W. Feng, E. Sun, A. Fujii, H. Wu, K. Nihara, K. Yoshino, Bull. Chem. Soc. Jpn. 73 (2000) 2627–2633.
[25] J.P. Pouget, M.E. Jozefowicz, A.J. Epstein, X. Tang, A.G. MacDiarmid, Macromolecules 24 (1999) 779–789.
[26] P.M. Kulal, D.P. Dubal, C.D. Lokhande, V.J. Fulari, J. Alloy. Compd. 509 (2011) 2567–2571.
[27] C.C. Hu, J.Y. Lin, Electrochim. Acta 47 (2002) 4055–4067.
[28] A.S. Aricò, P. Bruce, B. Scrosati, J.-M. Tarascon, W.V. Schalkwijk, Nat. Mater. 4 (2005) 366–377.
[29] A. Paulenova, S.E. Creager, J.D. Navratil, Y. Wei, J. Power Sources 109 (2002) 431–438.